Article type : Articles

Title: Limitations to recovery following wildfire in dry forests of southern Colorado and northern New Mexico, USA

Authors: Kyle C. Rodman[1,†], Thomas T. Veblen[1], Teresa B. Chapman[1,2], Monica T. Rother[3], Andreas P. Wion[4], and Miranda D. Redmond[4]

[1] Department of Geography, University of Colorado, Boulder, CO, 80309 USA

[2] The Nature Conservancy, Boulder, CO, 80302 USA

[3] Department of Environmental Studies, University of North Carolina, Wilmington, NC, 28403 USA

[4] Department of Forest and Rangeland Stewardship, Colorado State University, Fort Collins, CO, 80524 USA

[†] Corresponding author; email: kyle.rodman@colorado.edu

Running Head: Limitations to post-fire recovery

This article has been accepted for publication and undergone full peer review but has not been through the copyediting, typesetting, pagination and proofreading process, which may lead to differences between this version and the Version of Record. Please cite this article as doi: 10.1002/eap.2001

Abstract

Climate warming is contributing to increases in wildfire activity throughout the western U.S., leading to potentially long-lasting shifts in vegetation. The response of forest ecosystems to wildfire is thus a crucial indicator of future vegetation trajectories, and these responses are contingent upon factors such as seed availability, interannual climate variability, average climate, and other components of the physical environment. To better understand variation in resilience to wildfire across vulnerable dry forests, we surveyed conifer seedling densities in 15 recent (1988-2010) wildfires and characterized temporal variation in seed cone production and seedling establishment. We then predicted post-fire seedling densities at a 30-m resolution within each fire perimeter using downscaled climate data, monthly water balance models, and maps of surviving forest cover. Widespread ponderosa pine (*Pinus ponderosa*) seed cone production occurred at least twice following each fire surveyed, and pulses of conifer seedling establishment coincided with years of above-average moisture availability. Ponderosa pine and Douglas-fir (*Pseudotsuga menziesii*) seedling densities were higher on more mesic sites and adjacent to surviving trees, though there were also important interspecific differences, likely attributable to drought- and shade-tolerance. We estimated that post-fire seedling densities in 42% (for ponderosa pine) and 69% (for Douglas-fir) of the total burned area were below the lowest reported historical tree densities in these forests. Spatial models demonstrated that an absence of mature conifers (particularly in the interior of large, high-severity patches) limited seedling densities in many areas, but 30-year average actual evapotranspiration and climatic water deficit limited densities on marginal sites. A better understanding of the limitations to post-fire forest recovery will refine models of vegetation dynamics and will help to improve strategies of adaptation to a warming climate and shifting fire activity.

Key Words: Wildfire, Seed Production, Seedling Establishment, Dry Forests, Regeneration, Conifer, Ponderosa Pine, Douglas-fir, Climate Filtering, Fire Severity

Introduction

Over the past several decades, global-scale climate warming and extreme drought events have promoted increases in wildfire activity across a range of forest ecosystem types (Kasischke and Turetsky 2006, Brando et al. 2014, Singleton et al. 2018). Wildfire activity, in combination with the effects of warmer and drier conditions on tree regeneration processes, is increasing the potential for widespread forest losses (Enright et al. 2015, Stevens-Rumann et al. 2018). The rate of forest recovery following wildfire is a crucial parameter that controls the susceptibility of forests to type conversion (Tepley et al. 2018), and in dry coniferous forests of the western U.S. (i.e., lower-elevation forests with a dominant component of ponderosa pine [*Pinus ponderosa*]), early post-fire recovery differs drastically across biophysical gradients (Chambers et al. 2016, Rother and Veblen 2016, Kemp et al. 2019). Thus, forest resilience (*sensu* Holling 1973) to wildfire is also likely to vary across complex mountainous landscapes. Spatially-explicit predictions of post-fire forest recovery (e.g., Tepley et al. 2017, Haffey et al. 2018, Shive et al. 2018) can provide insight into relative differences in forest resilience across gradients in climate and fire severity.

The empirical assessment of drivers of tree regeneration (e.g., seed production, seedling germination, site suitability) will help to identify key bottlenecks to forest persistence in a warmer, drier future (Enright et al. 2015, Davis et al. 2018b). For the successful establishment of seed-obligate conifers (i.e., those incapable of vegetative reproduction) following wildfire, viable seed must be available in sites that are suitable for germination and survival. Together, these processes define the regeneration niche (*sensu* Grubb 1977), which has a tremendous influence on the distribution of forests. Following recent wildfires throughout the western U.S., it has been noted that seedling densities of non-serotinous conifers (i.e., trees without fire-adapted canopy seedbanks) are highest near surviving trees (Haire and McGarigal 2010, Chambers et al. 2016, Kemp et al. 2016, Tepley et al. 2017) due, in part, to greater seed availability. While seed dispersal is also influenced by tree height, seed characteristics, wind speed, and animal transport, seed availability is typically highest in close proximity to mature trees (McCaughey et al. 1986). This spatial component is well-documented, yet temporal variability in seed cone production of many conifers is poorly understood because the quantification of interannual variability in seed cone production requires either long-term monitoring or reconstruction based on persistent reproductive structures (*sensu* Forcella 1981). Information regarding ponderosa pine seed cone production is available in portions of the species' range throughout the western U.S. (e.g., Burns and Honkala 1990, Krannitz and Duralia 2004, Shepperd et al. 2006, Mooney et al. 2011, Keyes and Manso 2015), but strikingly little is known about seed cone production in post-fire landscapes. This knowledge is critical for a comprehensive examination of seed availability and its influence on tree regeneration.

Overstory forest cover and post-fire vegetation also have the potential to influence conifer establishment, growth, and survival through competition, facilitation, and microclimate modification. In mixed-species systems in which conifers coexist with resprouting angiosperm species, the post-fire cover of resprouting vegetation (shrubs and trees) typically increases with fire severity (Welch et al. 2016). Competing vegetation can reduce the growth rates of some conifers (Tepley et al. 2017) and may also inhibit seedling establishment, particularly for species such as ponderosa pine that regenerate well on bare mineral soil (Pearson 1942, Schubert 1976). Overstory forest cover modifies the understory environment by altering light availability (Battaglia et al. 2002) and by moderating daily maximum temperatures and diurnal fluctuations (Davis et al. 2018a). These buffering effects have the potential to reduce the influence of climate variability on seedlings, particularly for more shade-tolerant tree species capable of establishing and surviving within densely-forested sites (Dobrowski et al. 2015). Therefore, severe wildfire can reduce the potential for conifer seedling establishment by removing seed sources, altering the competitive environment, and eliminating the microclimatic buffering effects of the canopy.

In dry forests of the western U.S., post-fire conifer seedling densities are typically greater on wetter sites such as north-facing slopes and higher elevations (Dodson and Root 2013, Rother and Veblen 2016, Tepley et al. 2017, Haffey et al. 2018, Shive et al. 2018, Kemp et al. 2019). Post-fire recovery in conifer forests is also influenced by multiyear periods of drought and by interannual climate variability. For example, recovery is less likely in fires that are followed by abnormally dry periods (Harvey et al. 2016, Stevens-Rumann et al. 2018, Davis et al. 2019). One plausible mechanism creating these patterns is that seedling establishment for some montane conifer species is more likely in infrequent years with above-average moisture (Savage et al. 1996, League and Veblen 2006, Rother and Veblen 2017, Davis et al. 2019). Douglas-fir (*Pseudotsuga menziesii*) and ponderosa pine seedling survival is also greater under cool and moist conditions (Rother et al. 2015), with extreme drought years of particular importance to regeneration failure (Young et al. 2019).

An improved understanding of the potential limitations to post-fire conifer regeneration requires a synthetic approach that considers seed production, seedling establishment, and site suitability (Davis et al. 2018b). At 15 recent (1988 to 2010) fire events, we characterized annual seed cone production, resprouting of angiosperm trees, and conifer seedling establishment. We then combined these data with surveys of post-fire density for seedlings of two dominant coniferous tree species (Douglas-fir and ponderosa pine) and investigated the relationships between key biophysical factors and post-fire seedling densities across the 15 fire events. Finally, we used these data to predict seedling densities throughout each fire perimeter to better infer landscape-scale patterns of conifer forest resilience to wildfire. Specifically, we asked: 1) *How do seed cone production, conifer seedling establishment, and angiosperm resprouting vary following each fire?* 2) *Which biophysical factors best predict stand-scale variability in post-fire conifer seedling density?* 3) *What percentage of each fire and of total burned area has recovered to meet seedling density thresholds consistent with historical tree densities? 4) What is the percentage of total burned area in which post-fire conifer seedling densities were limited by a lack of mature conifers following fire?*

Methods

Study Area and Site Selection

Our study sites include 15 recent (1988-2010) wildfires that occurred in dry forests of southern Colorado and northern New Mexico, USA (Table 1, Fig. 1). We selected these fires as a subset of all large (> 404 ha) wildland fires in the southern portion (< 38.5 degrees N) of the Southern Rocky Mountains Ecoregion occurring from 1984-2010 (Eidenshink et al. 2007). We limited fire selection using the following criteria: 1) vegetation type – fires must have occurred in areas with dominant components of pine-oak, ponderosa pine, or dry mixed-conifer vegetation types (Rollins 2009), 2) accessibility – fires must have occurred on accessible public land, or on large private parcels for which we were permitted access, and 3) fires must have had only minimal areas of overlap with other fire perimeters (i.e., “reburns”). Out of the 41 wildfires meeting each of these criteria, we selected and were granted permission to sample in 15. Fire severity, area burned, pre-fire vegetation (Table 1), and average climate varied across the fires studied. Within fire perimeters, average January minimum temperatures range -14.9 to -6.8 C° and average July maximums range 18.1 to 30.2 C°. Total annual precipitation ranges 351 to 1049 mm, with a pronounced dry period in early summer (June and early July). Late-summer monsoons (mid-July to September) vary in importance across the study area and account for 30-45% of average annual precipitation, with increasing monsoonal contributions to the south and east (1981-2010 normals from the Parameter-Elevation Regression on Independent Slopes Model; PRISM 2018).

Regeneration Plots and Biophysical Predictors

For field surveys of post-fire conifer recovery, densities of resprouting angiosperms, and biophysical factors potentially influencing post-fire vegetation trajectories, we used a nested plot design with 8-12 transects within each fire perimeter and 3-6 plots along each transect. To identify the start of each transect, we first identified contiguous areas of low-, moderate-, and high-severity fire using thematic maps of dNBR (differenced Normalized Burn Ratio)-derived fire severity from the Monitoring Trends in Burn Severity project (Eidenshink et al. 2007). To locate each transect within a relatively homogenous area, we selected potential sites as contiguous patches of each severity class that exceeded 300 m in diameter. We excluded any areas with reforestation activities from site selection. Next, we created an accessibility layer in which we identified areas within each fire that were between 100 and 500 m of a system road or major trail. Finally, we identified 3-4 patches of each fire severity class that intersected the accessibility layer and spanned the geographic extent of the fire. We randomly located transect starts within each selected patch. Along each transect, we established plots with a 60-m systematic spacing and random offsets (10 m at a random azimuth). We allowed the number of transects and plots to vary within each fire perimeter based on the number of suitable patches identified, with the goal of establishing a total of 40 plots per fire (total n = 555).

Following Harvey et al. (2016), we used a variable-sized plot design to survey post-fire densities of conifer seedlings and resprouting angiosperms. Plot sizes were species-specific and based on initial surveys of abundance in each plot. For tree species with fewer than 25 post-fire stems within the full 15-m radius circular plot (707 m^2), we surveyed all stems. If more than 25 stems of a species were present in the full plot, sampling areas were reduced to the following: 25-100 stems - 120 m^2, 101-500 stems - 30 m^2, > 500 stems - 10 m^2. We defined seedlings as all conifers establishing following fire (as determined from bud scars [*sensu* Urza and Sibold 2013] and ring counts from increment cores), but we did not survey first-year germinants because of the high mortality rates for these individuals. Because seedling ages derived from bud scars can underestimate true seedling ages (Hankin et al. 2018), we may have slightly overestimated post-fire seedling densities in some low- and moderate-severity plots. However, these biases are greater for older and larger seedlings, for which we also used increment cores to verify ages.

To develop field-derived estimates of fire severity and to quantify pre- and post-fire forest structure, we recorded the species and diameter at breast height (1.37 m above ground level; DBH) of all live and dead overstory trees within each plot that likely pre-dated each fire. We determined pre-fire status of trees using stem diameter (> 10 cm DBH for conifers and > 5 cm for angiosperms; Table 2), level of decay, and char characteristics. We then estimated the relative dominance of ponderosa pine, Douglas-fir, and Gambel oak (*Quercus gambelii*) within each fire as the percentage of total pre-fire basal area in regeneration plots that was attributed to each species. We used branch morphology, wood characteristics, and the color and texture of remaining bark to identify the species of each dead individual. At the plot-level, we calculated the total pre-fire basal area of all species as a potential indicator of site productivity. We calculated field-derived fire severity as the percentage of total pre-fire basal area killed ~~on each plot~~ during the fire. At each plot center, we recorded the distance to the closest surviving mature conifer using a laser rangefinder. If these distances exceeded 500 m (the distance limitation of the instrument) or if ~~trees were not~~ visible from plot center, we measured the distance from plot center to the closest mature conifer using 2014 or 2015 aerial imagery (USFS 2015). Lastly, we quantified ground cover on each plot using four 1-m^2 quadrats and noted any evidence of grazing or browse damage by cattle or other ungulates (Table 2).

To quantify 30-year average and 3-year post-fire climate in each regeneration plot and within each fire perimeter, we performed a statistical downscaling (following Nalder and Wein 1998) of 30-year monthly averages of precipitation and temperature (i.e., 30-year normals), as well as monthly data from the fire year and each of the three years following the fire (PRISM 2018). Using these data, we modeled actual evapotranspiration (AET) and climatic water deficit (CWD) using a modified Thornthwaite-type method (Appendix S1; Lutz et al. 2010). We summed monthly values to calculate accumulated annual totals (by calendar year) of AET and CWD in each 30-m cell. We then developed predictors of 1) 30-year annual average AET and CWD, 2) 3-year average post-fire AET and CWD, and 3) the difference between 3-year average post-fire values and 30-year averages (Table 2). While CWD provides an estimate of the intensity of drought stress because it estimates unmet atmospheric moisture demand, AET is an indicator of site productivity because high values are indicative of sites with high availability of both moisture and energy (Dobrowski et al. 2015).

As an alternative to field-derived distances to mature conifers that could be characterized throughout each fire perimeter, we quantified post-fire canopy cover of mature conifers using image processing (following Rodman et al. 2019b) and classification of 1-m aerial imagery from the National Agriculture Imagery Progam (USFS 2015; Appendix S2). Overall accuracy of this classification was 90.2% at the level of a 1-m pixel (Appendix S2: Table S1). We aggregated the 1-m thematic maps to a 30-m resolution by extracting the percent cover of mature conifers in circular areas of different sizes (30-600 m radii in 30-m increments) surrounding each regeneration plot to assess the influences of post-fire canopy cover at multiple spatial scales.

Seed Cone Production

To characterize interannual variability in ponderosa pine seed cone production, we used the cone abscission scar method (Forcella 1981, Redmond et al. 2016). We performed these surveys within eight of the 15 fires, a subset that we selected to span the geographic and climatic ranges of our sites. Within each of these eight fires, we reconstructed seed cone production in at least two stands (27 stands total) and 4-6 trees/stand (154 total trees). Most stands were in close proximity (< 1 km) to post-fire regeneration plots, either in surviving stands within fire perimeters or in adjacent unburned areas. Following Redmond et al. (2016), we reconstructed seed cone production on 6-8 branches per tree by recording cone scars and remaining cones and conelets at each annual bud scar from 2003-2017. We counted the total number of cone bearing branches on each tree to scale our estimates of cones per branch to cones per tree. For individual trees, we defined seed cone years as years in which at least 25 cones were produced. Within fires, years of widespread seed cone production were defined as years in which at least 50% of trees produced more than 25 cones. To quantify synchrony in cone production, we calculated pairwise Spearman correlation coefficients (of seed cone counts by year)

~~between~~ all trees surveyed for seed cone production (following Mooney et al. 2011). To determine scales of synchrony, we then calculated the mean pairwise correlations of seed cone production for all trees (across fires), for trees within each fire (within fires), and for trees within individual stands.

Conifer Seedling Establishment and Angiosperm Resprouting

To describe temporal variability in conifer establishment and angiosperm resprouting following each fire, we collected up to two destructive samples of post-fire stems in each regeneration plot (total n = 696 successfully dated). If present, Douglas-fir, ponderosa pine, or lodgepole pine seedlings were excavated below soil level. If these coniferous species were absent, we harvested angiosperm (i.e., aspen [*Populus tremuloides*], Gambel oak) stems. We followed the lab protocols of Telewski (1993) and Rother and Veblen (2017) to identify the establishment year of conifers. From each conifer seedling, we cut and dated four cross-sections at varying stem heights. We then identified the establishment year as the innermost ring in the cross-section at, or immediately above, the root-shoot boundary. While time consuming, these methods are a notable improvement over node counts for the quantification of temporal trends in establishment (Hankin et al. 2018). For angiosperm stems, we determined the year of stem initiation from a single cross section near ground level. This likely approximates annual resolution given the rapid growth of these stems in the first few years after stem initiation.

We identified annual pulses of establishment for ponderosa pine and Douglas-fir at the regional-scale. First, we developed a single time series of seedlings dated to each year (1988-2015) by aggregating annual counts across fires. Next, we used a modified version of CharAnalysis (*sensu* Andrus et al. 2018) to detect pulses in this time series. CharAnalysis is an algorithm that identifies significant local outliers in time series data using a combination of non-linear detrending and Gaussian mixture models (Higuera et al. 2010, Tepley and Veblen 2015). For parameters in CharAnalysis, we used a five-year window width and a 90th percentile probability threshold. Following pulse detection, we qualitatively compared pulse years with interannual climate variables believed to influence tree establishment. Because moisture during the growing season may benefit conifer seedling establishment (Rother and Veblen 2017), we calculated accumulated climatic water deficit (CWD; Appendix S1) for April-September of each year (1981-2015) within each fire perimeter. We then calculated the mean value of April-September CWD from all grid cells within the 15 fire perimeters, and standardized yearly values through time to the series-wide mean and standard deviation (hereafter "z-scores"). Similarly, El Niño events (i.e., the warm phase of the El Niño Southern Oscillation [ENSO]) have been associated with episodic conifer establishment in the Southern Rocky Mountains (League and Veblen 2006), perhaps because of increases in winter precipitation during these years (Kurtzman and Scanlon 2007). Therefore, we obtained a Multivariate ENSO Index (MEI; Wolter and Timlin 2011) for the two month period of January-February (following League and Veblen 2006).

Seedling Density – Statistical Modeling

To develop statistical models of post-fire seedling densities for ponderosa pine and Douglas-fir, we used generalized linear mixed models (GLMMs; *sensu* Bolker et al. 2009) in the "glmmTMB" package (Brooks et al. 2017) in R (R Core Team 2018). Potential predictors in each GLMM included factors related to 30-year average climate, 3-year post-fire climate, fire severity, topography/terrain, herbivory, recovery of other tree species, pre-fire forest structure, and post-fire groundcover (Table 2). All spatially-extensive predictors were obtained or created at a 30-m resolution. We converted all continuous predictors to z-scores prior to model fitting to facilitate direct comparison of standardized model coefficients and to improve model stability. For GLMMs, we included data from the 555 regeneration plots across the 15 surveyed fires. Because of the hierarchical structure of data collection, we used nested random intercepts (transect within fire) to account for spatial dependence of plot data within each transect and across each fire. Semivariograms of model residuals indicated very little spatial dependence with this random effect structure (nugget:sill ratio near 1; Bivand et al. 2013). To account for differences in sampling area among plots (due to the variable-sized subplots used in this study), we also included an offset term of "log(subplot area)" for each species on each plot (Zuur et al. 2009). Following the development of initial zero-inflated GLMMs with a Poisson error structure, we used simulation-based tests of model residuals in the "DHARMa" package (Hartig 2018) in R to examine issues of dispersion. Our initial models were underdispersed and we therefore used a generalized Poisson error structure – a preferred distribution in these cases (Hilbe 2014).

We performed variable selection for our GLMMs of post-fire seedling density using an information-theoretic approach (Burnham and Anderson 2002). First, we fit initial models by developing GLMMs that included all potential predictors (Table 2) with the exception of those in highly correlated groups (e.g., groundcover, post-fire canopy cover of mature conifers in different radii). We then independently added predictors from each correlated group and used AIC (Akaike Information Criterion) to identify specific predictors in each group with the greatest explanatory power. After including these predictors, we then performed variable selection for final GLMMs by minimizing AIC while also balancing parsimony - in the case of two models with relatively similar AIC (i.e., ΔAIC < 2), we selected the simpler model. To assess final model ~~fit~~, we used a k-fold cross-validation procedure in which each GLMM was fit with the majority of the data, while plots from a single transect were withheld as the test set. We repeated this process with each transect (143 folds). We were interested in the ability of models to predict seedling densities that exceeded different density thresholds (see *Seedling Density—Spatial Modeling).* Therefore, we used balanced classification accuracy, a metric that evenly weights sensitivity and specificity, to quantify agreement between observed and predicted values in cross-validation.

Seedling Density – Spatial Modeling

We developed spatially-explicit predictions of ponderosa pine and Douglas-fir seedling densities at a 30-m resolution (hereafter "grid cells") within each of the 15 fire perimeters with an additional set of GLMMs, using only predictors that ~~were~~ characterized across the ~~entire area~~ of each fire (Table 2). This was done by conducting GLMM analyses similar to those described in *Seedling Density – Statistical Modeling*, but excluding variables of groundcover, pre-fire forest structure, local vegetation characteristics, and field-derived distances to mature conifers (Table 2). These GLMMs were then used to predict post-fire seedling densities in each grid cell throughout each fire (hereafter "spatial models"). Because Douglas-fir was only a minor component (< 10% basal area) of pre-fire basal area in five fires (Table 1), we excluded these fires from summaries of spatial model results for this species. We present results of spatial models for each fire, the total fire area (summed across all fires), and the total high-severity area (38.7% of total fire area). To identify these high-severity areas (i.e., grid cells with total canopy mortality), we used field-derived fire severity (percent basal area mortality) to train a classification ~~using~~ Landsat-derived RdNBR (relative differenced normalized burn ratio; Miller et al. 2009). Balanced accuracy of this classification was 84.4%.

From the spatial model predictions, we quantified the percentage of each fire, of total fire area, and of total high-severity area that exceeded density thresholds of 25 ponderosa pine seedlings ha^{-1} and 10 Douglas-fir seedlings ha^{-1}. These values correspond to some of the lowest reported stand densities in historical reconstructions of ponderosa pine and dry mixed-conifer forests throughout southern Colorado and the Southwest (Reynolds et al. 2013, Rodman et al. 2017). In order to identify sites most at risk of fire-facilitated conversion we used these thresholds as a broad/general approach to resilience. We acknowledge that the use of these universally low density thresholds as a means of assessing recovery from wildfire ignores the inherent variability in pre-fire density and species composition within and among fires. We tested the sensitivity of model results and classification accuracies to different tree density thresholds; the 25 and 10 seedlings ha^{-1} thresholds, for ponderosa pine and Douglas-fir, respectively, yielded the highest balanced accuracies of those tested (Appendix S3: Table S1, Appendix S3: Table S2). To describe potential drivers of variability among fires in these models, we calculated Spearman rank correlation coefficients between the percentage of each fire exceeding density thresholds and fire-level variables of: 1) percentage of area within each fire perimeter with total canopy mortality, 2) percentage of pre-fire basal area belonging to ponderosa pine or Douglas-fir, and 3) mean 30-year CWD within each fire perimeter.

Finally, to identify areas in which post-fire seedling densities of Douglas-fir and ponderosa pine were limited by the proximity to live conifers, we used the fitted GLMMs to predict seedling densities throughout each fire with observed climate surfaces (e.g., AET and CWD) and theoretically abundant canopy cover of mature conifers. We interpreted grid cells to be climatically suitable for seedlings but limited by the availability of surviving conifers if they were initially below the 25 and 10 seedlings ha^{-1} density thresholds with the observed post-fire canopy cover of mature conifers, but exceeded density thresholds given abundant canopy cover. Limitations to recovery in these grid cells likely reflect the combined influences of surviving forest cover on seed availability and on microclimatic buffering. We interpreted grid cells remaining below the 25 and 10 seedlings ha^{-1} density thresholds in both spatial models to have been limited by climatic predictors (e.g., AET, CWD) and/or fire-level random effects.

Results

Q1) *How do seed cone production, conifer seedling establishment, and angiosperm resprouting vary following each fire?*

While the abundance of ponderosa pine seed cone production varied through time and among the fires surveyed, we estimate that ponderosa pine seed was widely available in most areas with surviving mature trees (Fig. 2). From 2003-2017 (the range of years that could be reliably quantified using the cone abscission scar method), 74% of all surveyed trees had at least two seed cone years and 40% had at least five seed cone years (Fig. 2a). Each fire surveyed using the cone abscission scar method ($n = 8$) had multiple years of widespread seed cone availability following fire occurrence (Fig. 2b). These events occurred, on average, every 2-8 years. Seed cone production was asynchronous among fires (mean pairwise Spearman correlation; $\rho = 0.09$), though regionally important years occurred in 2006, 2009, 2012, 2015, and 2017 (Fig. 2c). Seed cone production was relatively synchronous within fires (mean $\rho = 0.25$, range = 0.08-0.40) and most synchronous within individual stands (mean $\rho = 0.38$, range = 0.02-0.64).

Lodgepole pine (which often have serotinous cones), as well as Gambel oak and aspen (which can resprout from established root systems following wildfire), showed abundant establishment immediately following individual fire events (Fig. 3). Specifically, 96% of lodgepole pine ~~samples~~ and 54% of oak and aspen stems were dated within three years of fire occurrence. Stems of resprouting angiosperms continued to initiate for many years after some fires (Fig. 3). Only 23% of ponderosa pine and Douglas-fir establishment occurred within three years of fire occurrence. Regional pulses of ponderosa pine and Douglas-fire seedling establishment, as identified through CharAnalysis, occurred in 1995, 1998, 2007, 2010, and 2014 (Fig. 4a). Three of the five pulses (1995, 1998, and 2007) took place during years with below-average CWD during the growing season (Fig. 4b), and four of the five pulses (1995, 1998, 2007, and 2010) were associated with El Niño events (i.e., a positive MEI in January and February; Fig. 4c). No strong temporal associations were evident between ponderosa pine seed cone production and seedling establishment at broad scales (Fig. 4d).

Q2) *Which biophysical factors best predict stand-scale variability in post-fire conifer seedling density?*

Final GLMMs of post-fire ponderosa pine seedling density – created using all field-derived and spatially-extensive variables as potential predictors – included 30-year average AET, 30-year average CWD, field-derived distances to mature conifers, percent basal area mortality, post-fire vegetation characteristics~~, and pre-fire basal area~~ (Fig. 5a). Low 30-year average CWD and high 30-year average AET, together indicative of productive areas with abundant moisture, were associated with higher seedling ~~desnities~~ (Fig. 5a). Interestingly, 30-year averages of CWD and AET were better predictors of ponderosa pine seedling density than were 3-year post-fire AET and CWD. Including 3-year post-fire climate variables did not improve predictive accuracy. Plots that were ~~both~~ adjacent to surviving mature conifers and burned at higher severity (i.e., greater percent basal area mortality) had higher densities of ponderosa pine~~, as indicated by the significant interaction between these two variables~~ (Fig. 5a). Grass cover and Gambel oak sprouting densities were negatively related to ponderosa pine density, while ~~pre-fire basal area and~~ post-fire Douglas-fir seedling density ~~were~~ positively related to ponderosa pine density (Fig. 5a). The Douglas-fir model with both field-derived and spatially-extensive variables did not improve upon the model including only spatially-extensive variables, thus we only present the latter model for Douglas-fir.

GLMMs developed for spatially-explicit models of ponderosa pine and Douglas-fir seedling densities were relatively similar to one another, including both 30-year average CWD and post-fire canopy cover of mature conifers as top predictors, but also had some important differences (Fig. 5b, 5c; Fig. 6). The ponderosa pine model included 30-year average CWD, 30-year average AET, and post-fire canopy cover of mature conifers, with 30-year CWD being the most important predictor. Low 30-year average CWD and high 30-year average AET were associated with higher ponderosa pine densities (Fig. 5b, Fig. 6b, Fig. 6c). The Douglas-fir model included only 30-year average CWD and post-fire canopy cover of mature conifers. Canopy cover was more important than was 30-year average CWD for Douglas-fir (Fig. 5c). The most notable difference between the two species was the relationship with post-fire canopy cover of mature conifers, which we assessed at a range of neighborhood sizes (30-600 m radii in 30-m increments). Ponderosa pine densities were highest in areas with intermediate (46%) canopy cover and the most influential neighborhood size was relatively broad: a 240-m radius (Fig. 5b, Fig. 6a). A non-linear term for canopy cover led to a slightly improved model fit (ΔAIC = 1.8) and a more ecologically realistic response given the shade-intolerant nature of ponderosa pine. In contrast, Douglas-fir densities were highest in dense stands (100% cover) and a localized 60-m neighborhood size was most influential (Fig. 5c, Fig 6d), consistent with overstory microclimatic buffering and the greater shade tolerance of this species.

While the GLMM of ponderosa pine density including all field-derived and spatially-extensive predictors had an improved fit when compared to the GLMM developed for spatially-explicit models (ΔAIC = 11.8), the differences in classification accuracy from cross-validation were relatively minor (71.8% balanced accuracy for the full model vs. 70.6% for the spatial model). For Douglas-fir, the GLMM used to inform spatial models had a balanced classification accuracy of 77.3%. Zero-inflation components of final GLMMs included only intercept terms and are not presented here.

Q3) *What percentage of each fire and of total burned area has recovered to meet seedling density thresholds consistent with historical tree densities?*

Spatially-explicit predictions of post-fire seedling densities for each species indicated that 42% and 69% of total fire area had ~~seedling~~ densities below 25 ponderosa pine and 10 Douglas-fir seedlings ha^{-1}, respectively (Fig. 7, Fig. 8). In the portions of these fires with total canopy mortality (high-severity), predicted densities were lower. We estimated that 57% of the total high-severity area did not exceed 25 ponderosa pine seedlings ha^{-1} and 79% of the total high-severity area did not exceed 10 Douglas-fir seedlings ha^{-1} (Appendix S3: Table S1, Appendix S3: Table S2).

Recovery also varied substantially among fires. For example, the Montoya Fire had 0% of total fire area exceeding 25 ponderosa pine and 10 Douglas-fir seedlings ha^{-1}, while the Saw Fire had 100% (ponderosa pine) and 98% (Douglas-fir) of fire area above these same density thresholds (Fig. 7, Fig. 8). The percentage of fire area exceeding density thresholds was positively correlated with pre-fire basal area for each species (ρ = 0.55 for ponderosa pine, ρ = 0.38 for Douglas-fir) and negatively correlated with the percentage of fire area with total canopy mortality (ρ = -0.50 for ponderosa pine, ρ = -0.52 for Douglas-fir). There were weaker relationships with mean 30-year CWD within fire perimeters (ρ = -0.15 for ponderosa pine, ρ = -0.25 for Douglas-fir). The percentage of fire area with total canopy mortality was not related to 30-year CWD (ρ = -0.01), and the 15 fires spanned broad ranges in both predictors.

Q4) *What is the percentage of total burned area in which post-fire conifer seedling densities were limited by a lack of mature conifers following fire?*

The drivers of limited conifer regeneration varied by species, within fire perimeters, and among fires. By substituting a theoretically-abundant canopy cover into our final models, we determined that 25% of total fire area was predicted to have less than 25 ponderosa pine seedings ha^{-1} due to a lack of mature conifers following fire (as measured through canopy cover in 1-m image classification; Appendix S3: Table S1). An additional 16% of fire area was predicted to be below 25 seedlings ha^{-1} (even with abundant canopy cover) due to 30-year average AET, 30-year average CWD, and random effects of fire (Appendix S3: Table S1). In contrast, Douglas-fir may be more strongly influenced by the canopy cover of mature conifers. For Douglas-fir, 68% of the total fire area was limited (below 10 seedlings ha^{-1}) by a lack of mature conifers (Appendix S3: Table S2).

Discussion

Limited recovery of seed-obligate conifers has been widely documented following recent wildfires throughout the western U.S. (e.g., Harvey et al. 2016, Rother and Veblen 2016, Shive et al. 2018, Stevens-Rumann et al. 2018, Kemp et al. 2019), yet the spatial and temporal variability in factors limiting post-fire forest recovery are still poorly understood. Building on the existing knowledge of recovery processes in dry forests, we note four key findings. First, our results indicate that seed cone production was not a major limitation to post-fire recovery of ponderosa pine. Second, five peak years of seedling establishment coincided with above-average moisture availability. Third, variability in post-fire conifer seedling density related to gradients in climate and fire severity, and seedling densities were highest on mesic sites and near surviving conifers. Fourth, Douglas-fir and ponderosa pine post-fire seedling densities were relatively low across a substantial percentage of the total burned area. Together, the initial filter of seed availability (a combination of seed production and proximity to mature conifers) and the secondary filter of climate limited conifer forest recovery across 15 recent wildfires in southern Colorado and northern New Mexico, USA.

Spatial and Temporal Limitations to Seed Availability and Other Effects of Live Trees

To date, little research has focused on the role of seed production in post-fire recovery of dry forests in the western U.S. In the present study, we found that the limited establishment of ponderosa pine following wildfires was not due to a lack of years of abundant seed cone production (i.e. mast years). Previous studies of seed cone production in ponderosa pine indicate that mast years may occur every 2-6 years (Maguire 1956, Krannitz and Duralia 2004, Shepperd et al. 2006), similar to our estimates of 2-8 years within fires. These findings have two important implications. First, the time interval between the initial disturbance and the time of our surveys was long enough to allow for at least one widespread ponderosa pine seed cone year in each fire. Second, given the relatively frequent seed cone production observed in this study, the patterns of surviving trees are a useful proxy for spatial variability in ponderosa pine seed availability throughout the landscape. Still, temporal variation in seed availability and alignment with climate conditions suitable for germination (*sensu* Savage et al. 1996, 2013, Petrie et al. 2017) is a poorly understood component of post-fire recovery needing additional research.

Fire severity, measured here using a combination of variables including field-derived distance to mature conifers, percent basal area mortality, post-fire canopy cover of mature conifers in aerial imagery, and satellite-derived RdNBR, was one of the factors best predicting post-fire ponderosa pine and Douglas-fir seedling densities. Fire severity ~~controls~~ the availability of live conifers throughout the landscape, which then drives spatial patterns of seed-availability. Surviving trees also modify temperature (Davis et al. 2018a), relative humidity (Paritsis et al. 2015), and light availability in the understory (Battaglia et al. 2002), thereby influencing seedling survival and resource availability in harsh post-fire environments. While canopy moderation may benefit both ponderosa pine and Douglas-fir, Douglas-fir is better adapted to benefit from microclimatic buffering (*sensu* Dobrowski et al. 2015) given its greater ability to tolerate the shaded understories of densely forested areas ~~(Bigelow et al. 2011)~~. For example, the areas predicted to have the highest densities of ponderosa pine seedlings were under intermediate levels of canopy cover (i.e., 46% in a 240-m radius). In contrast, Douglas-fir had higher seedling densities in dense stands (i.e., 100% cover in a 60-m radius). At a fine scale, we found that plots with high fire severity (as indicated by high percent basal area mortality), but in close-proximity to seed trees had high post-fire ponderosa pine seedling densities, likely due to fire-induced modifications of the seedbed and increased light availability on these sites (thus benefitting shade-intolerant ponderosa pine). Localized patches of high-severity fire may drive the abundant, aggregated establishment of ponderosa pine due to the presence of an adjacent seed source as well as bare mineral soil, available light, and increases in growing space (Sánchez Meador et al. 2009, Larson and Churchill 2012). Fire severity, influencing seed availability and conditions in the understory environment, is one of the most important factors limiting the recovery of seed-obligate conifers in post-fire environments.

Climate and Site Suitability as Constraints on Post-Fire Regeneration

Average climate (described by 30-year CWD and AET) was another strong predictor of post-fire densities for both ponderosa pine and Douglas-fir. Consistent with the findings of other studies (e.g., Dodson and Root 2013, Chambers et al. 2016, Kemp et al. 2016, Rother and Veblen 2016), we found that moisture-limited sites at low elevations and on southerly aspects typically had low conifer seedling densities, even in areas adjacent to a seed source. Many previous studies have utilized individual climate variables such as precipitation and temperature or terrain variables such as aspect and elevation to explain variability in post-fire conifer density. Water balance metrics such as CWD and AET provide a more useful alternative because they effectively combine the influence of climate, topography, and soils, and are functionally tied to the environmental conditions experienced by plants (Stephenson 1998, Dilts et al. 2015). When calculated at fine spatial resolutions that mirror the operational scales of post-fire recovery processes (as done in this study), AET and CWD are useful and complementary predictors of post-fire recovery in semi-arid landscapes and are helpful indicators of susceptibility to fire-driven conversions in vegetation.

Interestingly, 3-year post-fire CWD and AET had little predictive power in our seedling density models, yet post-fire climate has been noted as an influential driver of post-fire recovery in other studies (Harvey et al. 2016, Stevens-Rumann et al. 2018, Davis et al. 2019). A recent synthesis spanning much of the Rocky Mountains noted the post-fire climate was most predictive of forest recovery during cooler, wetter periods (Stevens-Rumann et al. 2018). Given that many of our fires occurred in the early-mid 2000s, a warm and dry period in which post-fire conditions may have been more universally unfavorable for seedlings, this is one possible explanation for differences between our findings and those of previous studies in regard to average post-fire conditions. In addition, we found that only 23% of ponderosa pine and Douglas-fir establishment occurred within three years of fire occurrence; interannual climate variability after the initial three-year post-fire period also plays an important role in post-fire vegetation trajectories.

At an annual resolution, extreme drought years influence longer-term forest trajectories, likely by increasing seedling mortality (Young et al. 2019), while wetter years lead to pulses of conifer establishment (Rother and Veblen 2017, Davis et al. 2019). Short-term (e.g., 3-5 years) averages of post-fire climate may mask the importance of these extreme years. In the present study, the 1995, 1998, 2007, 2010, and 2014 establishment pulses coincided with below-average CWD during the April-September growing season or with the warm (i.e. El Niño) phase of ENSO (which is associated with wet winters in the study area; Kurtzman and Scanlon 2007). Though these two components of interannual climate variability are generally related, they are not perfectly correlated (Fig. 4), and thus they represent slightly different seasonal effects that could influence establishment. For example, years with a positive MEI (El Niño conditions) may have above-average spring snowpack, yet may still accumulate CWD during the growing season due to above-average summer temperatures. Similar effects of interannual and sub-annual climatic variability are now well-documented in conifer forests throughout the southern Rocky Mountains and Southwest (Savage et al. 1996, League and Veblen 2006, Rother and Veblen 2017, Andrus et al. 2018, Davis et al. 2019). As such, demographic models that tie interannual climate variability to specific components of the conifer reproductive cycle are more informative than 3-5 year post-fire climatic averages (e.g., Feddema et al. 2013, Savage et al. 2013, Petrie et al. 2017, Davis et al. 2019). The consideration of longer time periods, both to assess the adequacy of recovery ~~(*sensu* Haire and McGarigal 2010)~~ and to identify potential windows for seedling establishment, is warranted in dry forests of the Southern Rocky Mountains.

Additional factors that helped to predict post-fire seedling densities included seedbed characteristics, post-fire recovery of other tree species, and pre-fire forest density. For example, our results indicated that grass cover and Gambel oak density both had negative relationships with ponderosa pine density at the stand-scale. Bunch grasses (e.g., *Festuca arizonica*) may compete with ponderosa seedlings for soil moisture (Pearson 1942), potentially limiting seedling densities (Flathers et al. 2016). In contrast to our findings, previous studies have noted that ponderosa pine may have weak (Owen et al. 2017) or even strong (Ziegler et al. 2017) positive spatial associations with resprouting angiosperm trees in post-fire environments. Gambel oak is believed to facilitate the establishment of another southwestern pine species (i.e., *Pinus edulis*; Floyd 1982) through microclimatic buffering and perhaps by attracting avian dispersers (such as corvids). Therefore, our finding of a negative relationship between Gambel oak density and ponderosa pine density may also reflect the occupancy of different site types rather than competitive or inhibitory interactions between these species. We also noted that high pre-fire basal area and post-fire Douglas-fir seedling density were positively related to ponderosa seedling density, perhaps indicative of wetter sites with better growing conditions. Post-fire seedling density is locally variable, reflecting variability in the seedbed, local vegetation characteristics, and growing conditions (as influenced by moisture availability and topoclimate).

Landscape-Scale Variability in Resilience to Fire

Spatial variability in conifer seedling density was effectively predicted throughout each fire using statistical models developed from field data and spatially-extensive datasets. Using these predictions, we determined that ponderosa pine and Douglas-fir regeneration was below the lowest reported historical tree densities in large percentages (42% and 69%, respectively) of the total area burned throughout 15 recent wildfires in southern Colorado and northern New Mexico, USA. Importantly, there was also pronounced variability in forest recovery among fires. Individual fire events ranged widely in post-fire recovery (with both species ranging from 0-100% across fires), which makes broad generalizations about causal mechanisms difficult. Still, much of this limited regeneration could be attributed to a lack of post-fire canopy cover of mature conifers and the unfavorable climate in portions of the surveyed sites (specifically 30-year average AET and CWD). In addition, recovery among fires was strongly related to differences in pre-fire species dominance, indicative of important legacy effects. Our spatial models provided an effective means of scaling stand-level observations to extensive post-fire landscapes (Tepley et al. 2017, Haffey et al. 2018, Shive et al. 2018), thus permitting broader inferences about vulnerability to post-fire vegetation type conversion.

Projections of future shifts from forest to non-forest vegetation types are inherently uncertain due to unknown future climatic variability as well as uncertainties about rates and specific drivers of vegetation change. Because our surveys were performed in relatively recent wildfires (1988-2010), it may be too early to suggest that transitions to non-forest vegetation types are permanent (Baker 2018). Still, the spatial variability in predicted densities across our study area indicates that some site types (e.g., xeric sites and those in the interior of high-severity patches) are more vulnerable to vegetation type conversions than others. Forest response to wildfire is often presented as a simplistic binary outcome of resilient versus non-resilient based on observations over periods of one to a few decades, yet a more nuanced approach to forest resilience considers rates of recovery, which can then create gradients of "relative resilience" across the landscape (Tepley et al. 2017, 2018, Shive et al. 2018). Given the importance of canopy cover and 30-year average CWD in predicting densities of both ponderosa pine and Douglas-fir, results from the current study imply that under continued warming and altered fire activity, some forested areas in the Southern Rocky Mountains are likely to undergo fire-driven conversions to non-forested vegetation (Parks et al. 2019).

Adaptation and Management Implications

Continued climate warming will increase the vulnerability of many low-elevation forests to conversion to non-forest vegetation types, and this presents complex challenges to land managers. Adequately addressing these challenges requires consideration of societal values and forest ecosystem services, as well as the best possible technical understanding of the potential for success of a variety of possible management interventions (Higuera et al. 2019). Potential management options include actions that attempt to forestall change through enhanced ecosystem resistance to fire effects, interventions aimed at improving post-fire resilience, and actions such as assisted migration aimed at facilitating ecosystem transformation to systems consistent with a changing climate (Millar et al. 2007, Halofsky et al. 2014). All management interventions have considerable risk due to uncertainties in predicting the rate and pattern of future climate change and the complexity of climate impacts on ecosystem dynamics. Therefore, a diverse range of approaches to adaptation and management should be considered (Millar et al. 2007, Baker 2018). Currently, reforestation is one of the most common management responses to large severe fires in the western U.S. (North et al. 2019), and the effectiveness of post-fire planting can vary widely (e.g., 0-70% survival in fires throughout Arizona and New Mexico; Ouzts et al. 2015). The likelihood of successful reforestation can benefit from the type of site-specific research on regeneration processes presented in the current study. If reforestation of recently-burned areas remains an important goal, relatively cool/wet sites should be prioritized first because seedling survival in these areas is likely to be greatest, now and into the future. Within these wetter areas, planting units should be limited to locations where available seed sources are most distant (Stevens-Rumann and Morgan 2019). The statistical analyses and spatial models presented here help to locate these types of sites in heterogenous burned landscapes by identifying areas that are climatically suitable, but in which recovery is limited by the proximity to live conifers. Our results are also important in informing discussions among stakeholders of the likelihood of future changes in the extent of forest cover, the probable changes in forest ecosystem services, and the costs and benefits of a range of adaptation strategies.

Conclusion

The factors limiting forest recovery to wildfire vary by species and across gradients in fire severity and climate. Because seed cone production was relatively frequent within each fire, the proximity to surviving conifers (as controlled by fire severity) is a reliable proxy for seed availability and is one of the most important factors driving post-fire recovery. Consistent with other recent studies (e.g., Dobrowski et al. 2015, Tepley et al. 2017), 30-year averages of actual evapotranspiration and climatic water deficit helped to quantify the climatic constraints on seedlings. In general, post-fire seedling densities of ponderosa pine and Douglas-fir were highest on wetter sites and near surviving trees. Anthropogenic climate change has led to increases in wildfire area burned throughout much of the western U.S. (Abatzoglou and Williams 2016) and these trends are likely to continue (Liu et al. 2013, Kitzberger et al. 2017), highlighting the importance of understanding the patterns of ecosystem recovery following these events. Post-fire recovery in dry forests is constrained by the initial filter of seed availability and the secondary filter of climatic suitability, together controlling the susceptibility to fire-driven forest losses.

Acknowledgments

This work was funded by Australian Research Council award DP170101288, Joint Fire Science Program Graduate Research Innovation award 17-2-01-4, the John Marr Ecology Fund, the Colorado Mountain Club Foundation, and the University of Colorado Boulder. Many thanks to Kelsey Bohanon, Aaron Broughton, Kristina Cowell, Molly Day, Katherine Feldmann, Angela Gonzalez, Ana Miller-ter Kuile, Josh Vonloh, Brenna Wider, and Jake Zatz for help with field data collection and laboratory work. Thanks also to Alan Tepley and Solomon Dobrowski for advice on ~~working with~~ climate data and water balance models. Numerous land managers working on the Santa Fe, Carson, San Juan, and Pike-San Isabel National Forests, as well as the Tercio, Trinchera-Blanca, and Vermejo Park ranches were integral to the success of this project by providing access to the research sites and by aiding in project planning. Lastly, we thank two anonymous reviewers for providing helpful feedback that improved this manuscript.

Literature Cited

Abatzoglou, J. T., and A. P. Williams. 2016. The Impact of Anthropogenic Climate Change on Wildfire Across Western US Forests. Proceedings of the National Academy of Sciences 113:11770–11775.

Andrus, R. A., B. J. Harvey, K. C. Rodman, S. J. Hart, and T. T. Veblen. 2018. Moisture Availability Limits Subalpine Tree Establishment. Ecology 99:567–575.

Baker, W. L. 2018. Transitioning Western U.S. Dry Forests to Limited Committed Warming with Bet-Hedging and Natural Disturbances. Ecosphere 9:e02288.

Battaglia, M. A., P. Mou, B. Palik, and R. J. Mitchell. 2002. The Effect of Spatially Variable Overstory on the Understory Light Environment of an Open-Canopied Longleaf Pine Forest. Canadian Journal of Forest Research 32:1984–1991.

~~Bigelow, S. W., M. P. North, and C. F. Salk. 2011. Using Light to Predict Fuels-Reduction and Group-Selection Effects on Succession in Sierran Mixed-Conifer Forest. Canadian Journal of Forest Research 41:2051–2063.~~

Bivand, R. S., E. Pebesma, and V. Gómez-Rubio. 2013. Applied Spatial Data Analysis with R. Springer, New York.

Bolker, B. M., M. E. Brooks, C. J. Clark, S. W. Geange, J. R. Poulsen, M. H. H. Stevens, and J.-S. S. White. 2009. Generalized Linear Mixed Models: A Practical Guide for Ecology and Evolution. Trends in Ecology & Evolution 24:127–135.

Brando, P. M., J. K. Balch, D. C. Nepstad, D. C. Morton, F. E. Putz, M. T. Coe, D. Silverio, M. N. Macedo, E. A. Davidson, C. C. Nobrega, A. Alencar, and B. S. Soares-Filho. 2014. Abrupt Increases in Amazonian Tree Mortality Due to Drought-Fire Interactions. Proceedings of the National Academy of Sciences 111:6347–6352.

Brooks, M. E., K. Kristensen, K. J. van Benthem, A. Magnusson, C. W. Berg, A. Nielsen, H. J. Skaug, M. Maechler, and B. M. Bolker. 2017. glmmTMB Balances Speed and Flexibility Among Packages for Zero-inflated Generalized Linear Mixed Modeling. The R Journal 9:378–400.

Burnham, K. P., and D. R. Anderson. 2002. Model Selection and Multimodel Inference: A Practical Information-Theoretic Approach. 2nd edition. Springer, New York.

Burns, R. M., and B. H. Honkala. 1990. Silvics of North America: Vol 1, Conifers. Agricultural Handbook 654. Washington, D.C.

Chambers, M. E., P. J. Fornwalt, S. L. Malone, and M. A. Battaglia. 2016. Patterns of Conifer Regeneration Following High Severity Wildfire in Ponderosa Pine – Dominated Forests of the Colorado Front Range. Forest Ecology and Management 378:57–67.

Davis, K. T., S. Z. Dobrowski, P. E. Higuera, Z. A. Holden, T. T. Veblen, M. T. Rother, A. Sala, and M. P. Maneta. 2019. Wildfires and Climate Change Push Low-Elevation Forests Across a Critical Climate Threshold for Tree Regeneration. Proceedings of the National Academy of Sciences 116:6193–6198.

Davis, K. T., S. Z. Dobrowski, Z. A. Holden, P. E. Higuera, and J. T. Abatzoglou. 2018a. Microclimatic Buffering in Forests of the Future: The Role of Local Water Balance. Ecography 42:1–11.

Davis, K. T., P. E. Higuera, and A. Sala. 2018b. Anticipating Fire-Mediated Impacts of Climate Change Using a Demographic Framework. Functional Ecology 32:1729–1745.

Dilts, T. E., P. J. Weisberg, C. M. Dencker, and J. C. Chambers. 2015. Functionally Relevant Climate Variables for Arid Lands: A Climatic Water Deficit Approach for Modelling Desert Shrub Distributions. Journal of Biogeography 42:1986–1997.

Dobrowski, S. Z., A. K. Swanson, J. T. Abatzoglou, Z. A. Holden, H. D. Safford, M. K. Schwartz, and D. G. Gavin. 2015. Forest Structure and Species Traits Mediate Projected Recruitment Declines in Western US Tree Species. Global Ecology and Biogeography 24:917–927.

Dodson, E. K., and H. T. Root. 2013. Conifer Regeneration Following Stand-Replacing Wildfire Varies Along an Elevation Gradient in a Ponderosa Pine Forest, Oregon, USA. Forest Ecology and Management 302:163–170.

Eidenshink, J., B. Schwind, K. Brewer, Z. Zhu, B. Quayle, S. Howard, S. Falls, and S. Falls. 2007. A Project for Monitoring Trends in Burn Severity. Fire Ecology 3:3–21.

Enright, N. J., J. B. Fontaine, D. M. J. S. Bowman, R. A. Bradstock, and R. J. Williams. 2015. Interval Squeeze: Altered Fire Regimes and Demographic Responses Interact to Threaten Woody Species Persistence as Climate Changes. Frontiers in Ecology and the Environment 13:265–272.

Feddema, J. J., J. N. Mast, and M. Savage. 2013. Modeling High-Severity Fire, Drought and Climate Change Impacts on Ponderosa Pine Regeneration. Ecological Modelling 253:56–69.

Flathers, K. N., T. E. Kolb, J. B. Bradford, K. M. Waring, and W. K. Moser. 2016. Long-Term Thinning Alters Ponderosa Pine Reproduction in Northern Arizona. Forest Ecology and Management 374:154–165.

Floyd, M. E. 1982. The Interaction of Piñon Pine and Gambel Oak in Plant Succession Near Dolores, Colorado. The Southwestern Naturalist 27:143–147.

Forcella, F. 1981. Estimating Pinyon Cone Production in New Mexico and Western Oklahoma. Journal of Wildlife Management 45:553–557.

Grubb, P. J. 1977. The Maintenance of Species-Richness in Plant Communities: The Importance of the Regeneration Niche. Biological Reviews of the Cambridge Philosophical Society 52:107–145.

Haffey, C., T. D. Sisk, C. D. Allen, A. E. Thode, and E. Q. Margolis. 2018. Limits to Ponderosa Pine Regeneration Following Large High-Severity Forest Fires in the United States Southwest. Fire Ecology 14:143–162.

Haire, S. L., and K. McGarigal. 2010. Effects of Landscape Patterns of Fire Severity on Regenerating Ponderosa Pine Forests (Pinus ponderosa) in New Mexico and Arizona, USA. Landscape Ecology 25:1055–1069.

Halofsky, J. S., J. E. Halofsky, T. Burcsu, and M. A. Hemstrom. 2014. Dry Forest Resilience Varies Under Simulated Climate-Management Scenarios in a Central Oregon, USA Landscape. Ecological Applications 24:1908–1925.

Hankin, L. E., P. E. Higuera, K. T. Davis, and S. Z. Dobrowski. 2018. Accuracy of Node and Bud-Scar Counts for Aging Two Dominant Conifers in Western North America. Forest Ecology and Management 427:365–371.

Hartig, F. 2018. Package ‘ DHARMa ’: Residual Diagnostics for Hierarchical (Mulit-Level/Mixed) Regression Models.

Harvey, B. J., D. C. Donato, and M. G. Turner. 2016. High and Dry: Postfire Drought and Large Stand-Replacing Burn Patches Reduce Postfire Tree Regeneration in Subalpine Forests. Global Ecology and Biogeography 25:655–669.

Higuera, P. E., D. G. Gavin, P. J. Bartlein, and D. J. Hallett. 2010. Peak Detection in Sediment Charcoal Records: Impacts of Alternative Data Analysis Methods on Fire-History. International Journal of Wildland Fire 19:996–1014.

Higuera, P. E., A. L. Metcalf, C. Miller, B. Buma, D. B. McWethy, E. C. Metcalf, Z. Ratajczak, C. R. Nelson, B. C. Chaffin, R. C. Stedman, S. McCaffrey, T. Schoennagel, B. J. Harvey, S. M. Hood, C. A. Schultz, A. E. Black, D. Campbell, J. H. Haggerty, R. E. Keane, M. A. Krawchuk, J. C. Kulig, R. Rafferty, and A. Virapongse. 2019. Integrating Subjective and Objective Dimensions of Resilience in Fire-Prone Landscapes. BioScience 69:379–388.

Hilbe, J. A. 2014. Modeling Count Data. Cambridge University Press, New York.

Holling, C. S. 1973. Resilience and Stability of Ecological Systems. Annual Review of Ecology and Systematics 4:1–23.

Kasischke, E. S., and M. R. Turetsky. 2006. Recent Changes in the Fire Regime Across the North American Boreal Region - Spatial and Temporal Patterns of Burning Across Canada and Alaska. Geophysical Research Letters 33:1–5.

Kemp, K. B., P. E. Higuera, and P. Morgan. 2016. Fire Legacies Impact Conifer Regeneration Across Environmental Gradients in the U.S. Northern Rockies. Landscape Ecology 31:619–635.

Kemp, K. B., P. E. Higuera, P. Morgan, and J. T. Abatzoglou. 2019. Climate Will Increasingly Determine Post-Fire Tree Regeneration Success in Low-Elevation Forests, Northern Rockies, USA. Ecosphere 10:e02568.

Keyes, C. R., and R. Manso. 2015. Climate-Influenced Ponderosa Pine (Pinus ponderosa) Seed Masting Trends in Western Montana, USA. Forest Systems 24:e021.

Kitzberger, T., D. A. Falk, A. L. Westerling, and T. W. Swetnam. 2017. Direct and Indirect Climate Controls Predict Heterogeneous Early-Mid 21st Century Wildfire Burned Area Across Western and Boreal North America. PLoS ONE 12:1–24.

Krannitz, P. G., and T. E. Duralia. 2004. Cone and Seed Production in Pinus ponderosa: A Review. Western North American Naturalist 64:208–218.

Kurtzman, D., and B. R. Scanlon. 2007. El Niño-Southern Oscillation and Pacific Decadal Oscillation Impacts on Precipitation in the Southern and Central United States: Evaluation of Spatial Distribution and Predictions. Water Resources Research 43:1–12.

Larson, A. J., and D. Churchill. 2012. Tree Spatial Patterns in Fire-Frequent Forests of Western North America, Including Mechanisms of Pattern Formation and Implications for Designing Fuel Reduction and Restoration Treatments. Forest Ecology and Management 267:74–92.

League, K. R., and T. T. Veblen. 2006. Climatic Variability and Episodic Pinus ponderosa Establishment Along the Forest-Grassland Ecotones of Colorado. Forest Ecology and Management 228:98–107.

Liu, Y., S. L. Goodrick, and J. A. Stanturf. 2013. Future U.S. Wildfire Potential Trends Projected Using a Dynamically Downscaled Climate Change Scenario. Forest Ecology and Management 294:120–135.

Lutz, J. A., J. W. van Wagtendonk, and J. F. Franklin. 2010. Climatic Water Deficit, Tree Species Ranges, and Climate Change in Yosemite National Park. Journal of Biogeography 37:936–950.

Maguire, W. P. 1956. Are Ponderosa Pine Cone Crops Predictable? Journal of Forestry 54:778–779.

McCaughey, W. W., W. C. Schmidt, and R. C. Shearer. 1986. Seed-Dispersal Characteristics of Conifers in the Inland Mountain West. Pages 50–62 in R. C. Shearer, editor. Conifer Tree Seed in the Inland Mountain West Symposium. Gen. Tech. Rep. INT-GTR-203. USDA Forest Service, Intermountain Research Station, Missoula, MT.

Millar, C. I., N. L. Stephenson, and S. L. Stephens. 2007. Climate Change and Forest of the Future: Managing in the Face of Uncertainty. Ecological Applications 17:2145–2151.

Miller, J. D., E. E. Knapp, C. H. Key, C. N. Skinner, C. J. Isbell, R. M. Creasy, and J. W. Sherlock. 2009. Calibration and Validation of the Relative Differenced Normalized Burn Ratio (RdNBR) to Three Measures of Fire Severity in the Sierra Nevada and Klamath Mountains, California, USA. Remote Sensing of Environment 113:645–656.

Mooney, K. A., Y. B. Linhart, and M. A. Snyder. 2011. Masting in Ponderosa Pine: Comparisons of Pollen and Seed Over Space and Time. Oecologia 165:651–661.

Nalder, I. A., and R. W. Wein. 1998. Spatial Interpolation of Climatic Normals: Test of a New Method in the Canadian Boreal Forest. Agricultural and Forest Meteorology 92:211–225.

North, M. P., J. T. Stevens, D. F. Greene, M. Coppoletta, E. E. Knapp, A. M. Latimer, C. M. Restaino, R. E. Tompkins, K. R. Welch, R. A. York, D. J. N. Young, J. N. Axelson, T. N. Buckley, B. L. Estes, R. N. Hager, J. W. Long, M. D. Meyer, S. M. Ostoja, H. D. Safford, K. L. Shive, C. L. Tubbesing, H. Vice, D. Walsh, C. M. Werner, and P. Wyrsch. 2019. Tamm Review: Reforestation for Resilience in Dry Western U.S. Forests. Forest Ecology and Management 432:209–224.

Ouzts, J. R., T. E. Kolb, D. W. Huffman, and A. J. Sánchez Meador. 2015. Post-fire Ponderosa Pine Regeneration With and Without Planting in Arizona and New Mexico. Forest Ecology and Management 354:281–290.

Owen, S. M., C. H. Sieg, A. J. Sánchez Meador, P. Z. Fulé, J. M. Iniguez, L. S. Baggett, P. J. Fornwalt, and M. A. Battaglia. 2017. Spatial Patterns of Ponderosa Pine Regeneration in High-Severity Burn Patches. Forest Ecology and Management 405:134–149.

Paritsis, J., T. T. Veblen, and A. Holz. 2015. Positive Fire Feedbacks Contribute to Shifts from Nothofagus pumilio Forests to Fire-Prone Shrublands in Patagonia. Journal of Vegetation Science 26:89–101.

Parks, S. A., S. Z. Dobrowski, J. D. Shaw, and C. Miller. 2019. Living on the Edge: Trailing Edge Forests at Risk of Fire-Facilitated Conversion to Non-Forest. Ecosphere 10:e02651.

Pearson, G. A. 1942. Herbaceous Vegetation a Factor in Natural Regeneration of Ponderosa Pine in the Southwest. Ecological Monographs 12:315–338.

Petrie, M. D., J. B. Bradford, R. M. Hubbard, W. K. Lauenroth, C. M. Andrews, and D. R. Schlaepfer. 2017. Climate Change May Restrict Dryland Forest Regeneration in the 21st Century. Ecology 98:1548–1559.

PRISM Climate Group, Oregon State University. 2018. <http://prism.oregonstate.edu>

R Core Team. 2018. R: A Language and Environment for Statistical Computing. R Foundation for Statistical Computing, Vienna, Austria.

Redmond, M. D., P. J. Weisberg, N. S. Cobb, C. A. Gehring, A. V Whipple, and T. G. Whitham. 2016. A Robust Method to Determine Historical Annual Cone Production Among Slow-Growing Conifers. Forest Ecology and Management 368:1–6.

Reynolds, R. T., A. J. Sánchez Meador, J. A. Youtz, T. Nicolet, M. S. Matonis, P. L. Jackson, D. G. Delorenzo, and A. D. Graves. 2013. Restoring Composition and Structure in Southwestern Frequent-Fire Forests: A Science-Based Framework for Improving Ecosystem Resiliency. RMRS GTR-310. Fort Collins, CO.

Rodman, K. C., A. J. Sánchez Meador, M. M. Moore, and D. W. Huffman. 2017. Reference Conditions Are Influenced by the Physical Template and Vary by Forest Type: A Synthesis of Pinus Ponderosa-Dominated Sites in the Southwestern United States. Forest Ecology and Management 404:316–329.

Rodman, K. C., T. T. Veblen, T. B. Chapman, M. T. Rother, A. P. Wion, and M. D. Redmond. 2019a. Data from: Limitations to Recovery Following Wildfire in Dry Forests of Southern Colorado and Northern New Mexico, USA. Dryad Digital Repository, doi:10.5061/dryad.t02nd5m.

Rodman, K. C., T. T. Veblen, S. Saraceni, and T. B. Chapman. 2019b. Wildfire Activity and Land Use Drove 20th Century Changes in Forest Cover in the Colorado Front Range. Ecosphere 10:e02594.

Rollins, M. G. 2009. LANDFIRE: A Nationally Consistent Vegetation, Wildland Fire, and Fuel Assessment. International Journal of Wildland Fire 18:235–249.

Rother, M. T., and T. T. Veblen. 2016. Limited Conifer Regeneration Following Wildfires in Dry Ponderosa Pine Forests of the Colorado Front Range. Ecosphere 7:e01594.

Rother, M. T., and T. T. Veblen. 2017. Climate Drives Episodic Conifer Establishment after Fire in Dry Ponderosa Pine Forests of the Colorado. Forests 8:159.

Rother, M. T., T. T. Veblen, and L. G. Furman. 2015. A Field Experiment Informs Expected Patterns of Conifer Regeneration After Disturbance Under Changing Climate Conditions. Canadian Journal of Forest Research 45:1607–1616.

Sánchez Meador, A. J., M. M. Moore, J. D. Bakker, and P. F. Parysow. 2009. 108 Years of Change in Spatial Pattern Following Selective Harvest of a Pinus Ponderosa Stand in Northern Arizona, USA. Journal of Vegetation Science 20:79–90.

Savage, M., P. M. Brown, and J. J. Feddema. 1996. The Role of Climate in a Pine Forest Regeneration Pulse in the Southwestern United States. Ecoscience 3:310–318.

Savage, M., J. N. Mast, and J. J. Feddema. 2013. Double Whammy: High-Severity Fire and Drought in Ponderosa Pine Forests of the Southwest. Canadian Journal of Forest Research 43:570–583.

Schubert, G. H. 1976. Silviculture of Southwestern Ponderosa Pine: The Status of Our Knowledge. Res. Pap. RM-123. Fort Collins, CO.

Shepperd, W. D., C. B. Edminster, and S. A. Mata. 2006. Long-Term Seedfall, Establishment, Survival, and Growth of Natural and Planted Ponderosa Pine in the Colorado Front Range. Western Journal of Applied Forestry 21:19–26.

Shive, K. L., H. K. Preisler, K. R. Welch, H. D. Safford, R. J. Butz, K. L. O'Hara, and S. L. Stephens. 2018. From the Stand-Scale to the Landscape-Scale: Predicting the Spatial Patterns of Forest Regeneration After Disturbance. Ecological Applications 28:1626–1639.

Singleton, M. P., A. E. Thode, A. J. Sánchez Meador, and J. M. Iniguez. 2018. Increasing Trends in High-Severity Fire in the Southwestern USA from 1984-2015. Forest Ecology and Management 433:709–719.

Stephenson, N. L. 1998. Actual Evapotranspiration and Deficit: Biologically Meaningful Correlates of Vegetation Distribution Across Spatial Scales. Journal of Biogeography 25:855–870.

Stevens-Rumann, C. S., K. B. Kemp, P. E. Higuera, B. J. Harvey, M. T. Rother, D. C. Donato, P. Morgan, and T. T. Veblen. 2018. Evidence for Declining Forest Resilience to Wildfires Under Climate Change. Ecology Letters 21:243–252.

Stevens-Rumann, C. S., and P. Morgan. 2019. Tree Regeneration Following Wildfires in the Western US: A Review. Fire Ecology 15:1–17.

Telewski, F. W. 1993. Determining the Germination Date of Woody Plants: A Proposed Method for Locating the Root/Shoot Interface. Tree-Ring Bulletin 53:13–16.

Tepley, A. J., E. Thomann, T. T. Veblen, G. L. W. Perry, A. Holz, J. Paritsis, T. Kitzberger, and K. J. Anderson-Teixeira. 2018. Influences of Fire-Vegetation Feedbacks and Post-Fire Recovery Rates on Forest Landscape Vulnerability to Altered Fire Regimes. Journal of Ecology 106:1925–1940.

Tepley, A. J., J. R. Thompson, H. E. Epstein, and K. J. Anderson-Teixeira. 2017. Vulnerability to Forest Loss Through Altered Postfire Recovery Dynamics in a Warming Climate in the Klamath Mountains. Global Change Biology 23:4117–4132.

Tepley, A. J., and T. T. Veblen. 2015. Spatiotemporal Fire Dynamics in Mixed-Conifer and Aspen Forests in the San Juan Mountains of Southwestern Colorado, USA. Ecological Monographs 85:583–603.

Theobald, D. M., D. Harrison-Atlas, and W. B. Monahan. 2015. Ecologically-Relevant Maps of Landforms and Physiographic Diversity for Climate Adaptation Planning. PLoS ONE 10:1–17.

United States Forest Service, National Agriculture Imagery Program. 2015. <http://www.fsa.usda.gov/programs-and-services/aerial-photography/imagery-programs/naip-imagery/>

Urza, A. K., and J. S. Sibold. 2013. Nondestructive Aging of Postfire Seedlings for Four Conifer Species in Northwestern Montana. Western Journal of Applied Forestry 28:22–29.

Welch, K. R., H. D. Safford, and T. P. Young. 2016. Predicting Conifer Establishment 5-7 years After Wildfire in Middle Elevation Yellow Pine and Mixed Conifer Forests of the North American Mediterranean-Climate Zone. Ecosphere 7:1–29.

Young, D. J. N., C. M. Werner, K. R. Welch, T. P. Young, H. D. Safford, and A. M. Latimer. 2019. Post-Fire Forest Regeneration Shows Limited Climate Tracking and Potential for Drought-Induced Type Conversion. Ecology 100:e02571.

Ziegler, J. P., C. Hoffman, P. Fornwalt, C. Sieg, M. A. Battaglia, and J. M. Iniguez. 2017. Tree Regeneration Spatial Patterns in Ponderosa Pine Forests Following Stand-Replacing Fire: Influence of Topography and Neighbors. Forests 8:391.

Zuur, A. F., E. N. Ieno, N. J. Walker, A. A. Saveliev, and G. M. Smith. 2009. Mixed Effects Models and Extensions in Ecology and R. Springer, New York.

Data Availability

Following a one-year embargo, data associated with this paper will be made available in the Dryad Digital Repository: http://dx.doi.org/10.5061/dryad.t02nd5m (Rodman et al. 2019a).

Table 1: Descriptions of the 15 surveyed fires in southern Colorado and northern New Mexico, USA. "Area" is the areal extent of mapped fire perimeters from the Monitoring Trends in Burn Severity program (Eidenshink et al. 2007). "High Severity" is the percentage of each fire that burned at high severity (total canopy mortality) based on satellite-derived burn severity classification with field validation. Pre-fire species composition, derived from field inventories of live and dead trees, is given for the three most prevalent species across sites (Douglas-fir, Gambel oak, and ponderosa pine) and represents the percentage of pre-fire basal area belonging to a given species in each fire.

Fire Summary Information					Pre-Fire Species Composition (% BA)			Plots
Fire Name	**Area (ha)**	**High Severity (%)**	**Year**	**Elevation Range (m)**	**Douglas-Fir**	**Gambel Oak**	**Ponderosa Pine**	**n**
Borrego	5,211	21	2002	2163-3111	11	< 1	72	40
H12	1,778	10	2010	2497-2964	18	2	77	40
Hondo	3,339	69	1996	2261-3605	11	< 1	59	31
Lakes	1,742	37	2002	2290-2673	43	< 1	39	40
Mason	4,461	70	2005	1861-2494	14	1	78	37
Mato Vega	5,312	61	2006	2568-3235	45	0	18	36
Missionary Ridge	27,891	34	2002	2010-3560	32	< 1	23	33
Montoya	1,666	45	2002	2437-2870	0	13	42	37
Pine Canyon	1,656	21	2005	2214-2645	0	3	70	36
Ponil Complex	36,051	32	2002	2027-2842	10	< 1	86	33
Saw	1,259	0	1988	2262-2485	12	10	82	38
Spring	9,730	49	2002	2316-2867	29	1	60	45
Viveash	9,093	63	2000	2418-3539	49	< 1	29	29
West Fork	2,200	15	2008	2196-2569	4	1	60	40
York	1,314	9	2001	2389-2800	6	3	85	40
All Fires	**Total Area: 112,703**	**% of Total: 39**	**Range: 1988-2010**	**Range: 1861-3605**	**% of Total: 23**	**% of Total: 2**	**% of Total: 56**	**Total: 555**

Table 2: Descriptions of predictor variables included in statistical models of post-fire seedling density for ponderosa pine and Douglas-fir across 15 fires in southern Colorado and northern New Mexico, USA. Expected relationships of each variable with ponderosa pine ("PIPO") and Douglas-fir ("PSME") densities are shown with (+) or (-). Spatially-extensive variables that could be used to inform spatial models of seedling densities within fire perimeters ("Spatial Model") are denoted with (x).

Category	Variable Name	Description	PIPO	PSME	Spatial Model
Average Climate	30-Year Average AET	Average actual evapotranspiration (AET; evaporative loss constrained by moisture availability) calculated at a monthly timestep from downscaled 30-year normals (1981-2010) and summed by calendar year.	+	+ or -	x
	30-Year Average CWD	Average climatic water deficit (CWD; the difference between potential and actual evapotranspiration) calculated at a monthly timestep from downscaled 30-year normals (1981-2010) and summed by calendar year.	-	-	x
Post-Fire Climate	3-Year Post-Fire AET	Average AET calculated from downscaled monthly data in the first three years after a fire. The mean of the three annual values.	+	+ or -	x
	3-Year Post-Fire CWD	Average CWD calculated from downscaled monthly data in the first three years after a fire. The mean of the three annual values.	-	-	x
	Post-Fire AET Deviation	Difference between 3-year post-fire AET and 30-year average AET.	+	+ or -	x
	Post-Fire CWD Deviation	Difference between 3-year post-fire CWD and 30-year average CWD.	-	-	x
Fire Severity	Canopy Cover of Mature	The percentage of total surface area surrounding each field plot classified as mature conifer cover in 1-m post-fire imagery.	+ or -	+	x

	Conifers	Calculated in 20 different neighborhood sizes (i.e., circular areas with radii of 30-600 m in 30-m increments).			
	Distance to Mature Conifer	Field-derived distance (m) from plot-center to nearest surviving conifer.	-	-	
	Percent BA Mortality	Field-derived percentage of pre-fire basal area killed during event.	+ or -	-	
	RdNBR	Landsat-derived fire severity index using pre- and post-fire imagery.	+ or -	-	x
Topography/ Terrain	Topographic Position Index	Index describing relative topographic position of each 30-m cell. High values are associated with ridgetops and low values are associated with valley bottoms.	+ or -	-	x
	Landform Classification	Categorical variable combining topographic position, aspect, and soils at 30-m resolution. From Theobald et al. (2015)	+ on intermediate slopes	+ on cool/wet slopes	x
Herbivory	Grazing/ Browsing	Binary variable (presence/absence) of cattle grazing or ungulate browse damage on each plot.	-	-	
Post-Fire Recovery of Other Tree Species	Douglas-Fir Seedling Density	Density (seedlings ha^{-1}) of post-fire Douglas-fir seedlings. Used only as predictor of ponderosa pine density.	+	N/A	
	Gambel Oak Sprout Density	Density (stems ha^{-1}) of post-fire Gambel oak.	+ or -	+	
	Other Conifer Seedling Density	Density (stems ha^{-1}) of post-fire conifers of other species (i.e., fir, spruce, lodgepole pine, pinyon pine, and juniper).	-	-	
Pre-Fire Forest Structure	Pre-Fire Basal Area	Combined basal area of live and dead overstory trees of all species in a given plot.	+	+	
Groundcover	Bare Ground	Percent cover of bare ground in 1-m^2 quadrats.	+	-	

/Seedbed					
	Percent Coarse Wood	Percent cover of coarse wood in 1-m^2 quadrats.	+	+	
	Percent Forb	Percent cover of forbs in 1-m^2 quadrats.	+	+	
	Percent Grass	Percent cover of graminoids in 1-m^2 quadrats.	-	+ or -	
	Percent Litter	Percent cover of litter in 1-m^2 quadrats.	-	+	
	Percent Rock	Percent cover of rock in 1-m^2 quadrats.	-	-	
	Percent Shrub	Percent cover of low (< 1.4 m in height) shrubs in 1-m^2 quadrats.	+ or -	+	

Figure Captions

Fig. 1. Map of the study area in southern Colorado and northern New Mexico, USA, showing the 15 wildfires surveyed for post-fire forest recovery. Green shading shows the distribution of forests based on the 1992 National Land Cover Dataset (NLCD), which preceded most of the wildfires surveyed.

Fig. 2. A summary of ponderosa pine seed cone production at (a) the tree level and (b, c) the fire level in eight surveyed fires in southern Colorado and northern New Mexico, USA. Tree-level production gives (a) the percentage of trees (across all sites; n = 154) exceeding different numbers of individual seed years (2003-2017), where seed years were defined as individual years with at least 25 seed cones produced. Fire-level production gives (b) the percentage (bar heights) and number of post-fire years (between fire occurrence and the time of surveys; numbers above each bar) with widespread seed cone production (at least 50% of surveyed trees recording seed years), as well as (c) the estimated annual cone production tree^{-1} within each fire. Bar colors and fire names in (b) match lines in (c). Cone production prior to 2003 could not be reliably quantified using the cone abscission scar method.

Fig. 3. Temporal patterns of conifer seedling establishment (for Douglas-fir, ponderosa pine, and lodgepole pine) and the timing of resprouting (for aspen and Gambel oak) across each of 15 surveyed fires in southern Colorado and northern New Mexico, USA. Counts are derived from destructive samples collected throughout each fire and dated with annual precision. Years of fire occurrence are shown with a triangle and dashed line. The total number of seedlings and stems aged in each fire is given by n. Information on pre-fire species composition and burn severity in each fire are provided in Table 1.

Fig. 4. A summary of conifer establishment, angiosperm resprouting, interannual climate variability (1988-2015), and ponderosa pine seed cone production across 15 surveyed fires in southern Colorado and northern New Mexico, USA. Destructively-sampled seedlings (conifers) and stems (angiosperms) were collected throughout each fire and (a) dated with annual precision. Bar colors correspond to each of the five sampled species, and bar heights correspond to the number of samples dated to each year.

Triangles and vertical dashed lines show significant pulses of ponderosa pine and Douglas-fir establishment (1995, 1998, 2007, 2010, and 2014) based on CharAnalysis – a pulse detection algorithm that identifies local outliers. Interannual climate variability was characterized with (b) CWD (climatic water deficit) during the growing season (April-September) and (c) the multivariate El Niño Southern Oscillation index (MEI). Lastly, (d) ponderosa pine establishment across all sites (green bars) is overlaid with the mean annual seed cone production tree^{-1} (in a subset of eight fires) in the year prior to seedling establishment (hollow circles).

Fig. 5. ~~Standardized coefficients and significance levels for each of the predictors included in generalized linear mixed models predicting postfire (a, b) ponderosa pine and (c) Douglas-fir seedling density. Error bars are ± one standard error of the coefficient estimate. Models were developed for ponderosa pine seedling density from (a) all potential predictors (both field-derived and the spatially-extensive variables), (b) ponderosa pine seedling density from spatially-extensive predictors only (for later use in spatial modeling) and (c) Douglas-fir seedling density from spatially-extensive predictors. We do not present a model for Douglas-fir seedling density using field-based predictors because these did not improve model fit. Coefficients are for the conditional models only and do not include zero-inflation terms or random intercept coefficients. Orthogonal polynomial terms (non-linear predictors) are given with the variable name preceded by "poly" and variable interactions are given by linking two variable names with "x".~~

Fig. 6. Results of generalized linear mixed models that were used to predict post-fire seedling densities of ponderosa pine and Douglas-fir across each of the surveyed fires in southern Colorado and northern New Mexico, USA. Predicted values (solid lines) represent the marginal effects of each predictor when assuming optimal values for the other predictors and mean values of random effects. Dotted lines are ± one standard error of prediction. Variables include (a, d) canopy cover - the percent surface area of mature conifers within a circular radius, (b, e) 30-year average CWD (climatic water deficit), and (c) 30-year average AET (actual evapotranspiration) – measures of unmet evaporative demand and evaporation constrained by moisture availability, respectively. Variation among fires is

shown with (f) random intercept coefficients for each species, where colors indicate positive (blue) or negative (red) deviations from the mean value across all sites.

Fig 7. Predicted ponderosa pine seedling densities throughout each surveyed fire in southern Colorado and northern New Mexico based on ~~the landscape GLMMs.~~ The percentage values in each panel give the percentage of fire area exceeding a density threshold of 25 seedlings ha^{-1}, which corresponds to some of the lowest historically reported densities for this species in ponderosa-pine dominated forests of the Southern Rocky Mountains and Southwest (Rodman et al. 2017). Blue areas in each map exceed this threshold while red areas are below this threshold. Note that cartographic scales differ among panels.

Fig. 8. Predicted Douglas-fir seedling densities throughout each surveyed fire in southern Colorado and northern New Mexico based on ~~the landscape GLMMs~~. The percentage values in each panel give the percentage of fire area exceeding a density threshold of 10 seedlings ha^{-1}, which corresponds to some of the lowest historically reported densities for this species in dry mixed-conifer forests of the Southern Rocky Mountains and Southwest (Rodman et al. 2017). Blue areas in each map exceed this threshold while red areas are below this threshold. Fire names followed by (*) are those in which Douglas-fir represented less than 10% of pre-fire basal area. These fires were excluded from summaries of spatial models. Note that cartographic scales differ among panels.

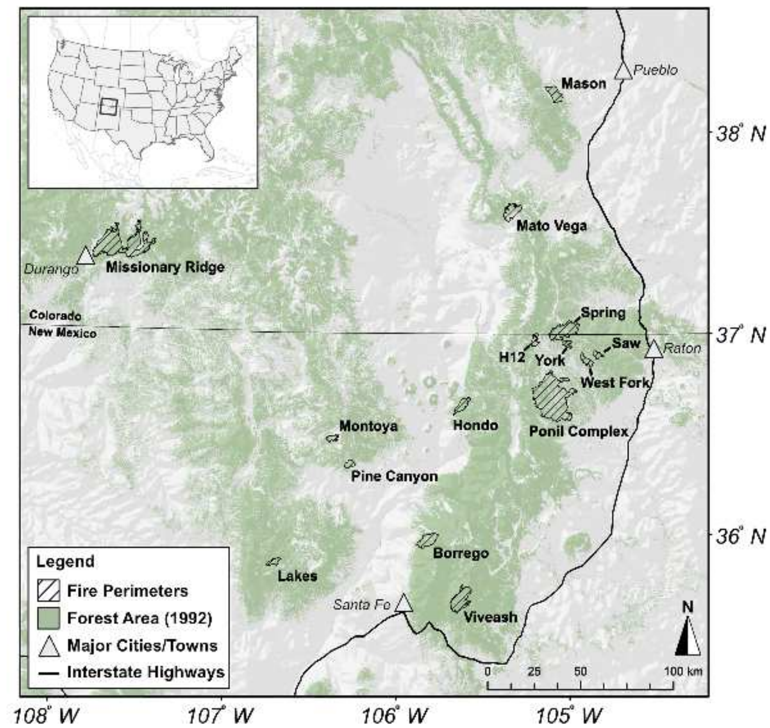

eap_2001_f1.tiff

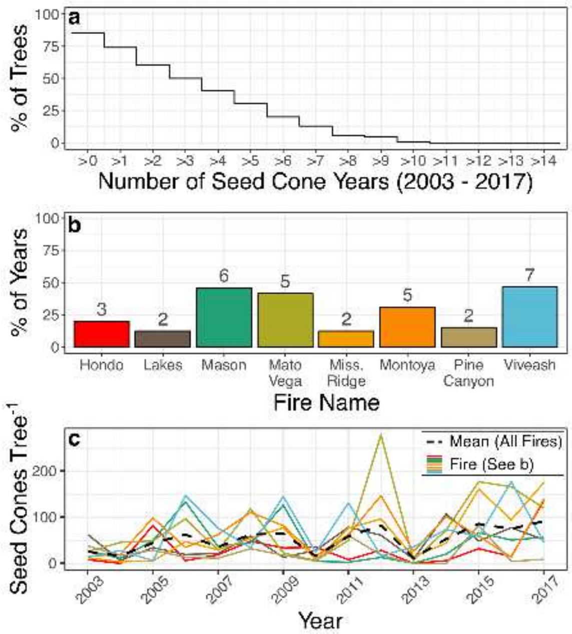

eap_2001_f2.tiff

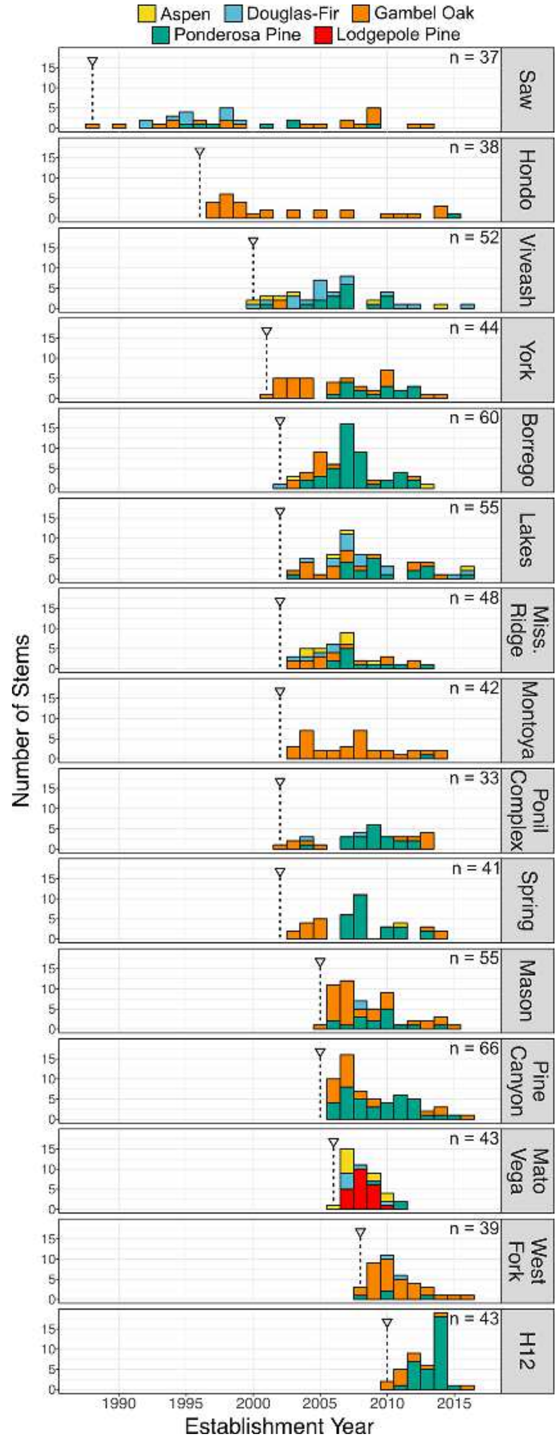

eap_2001_f3.tif

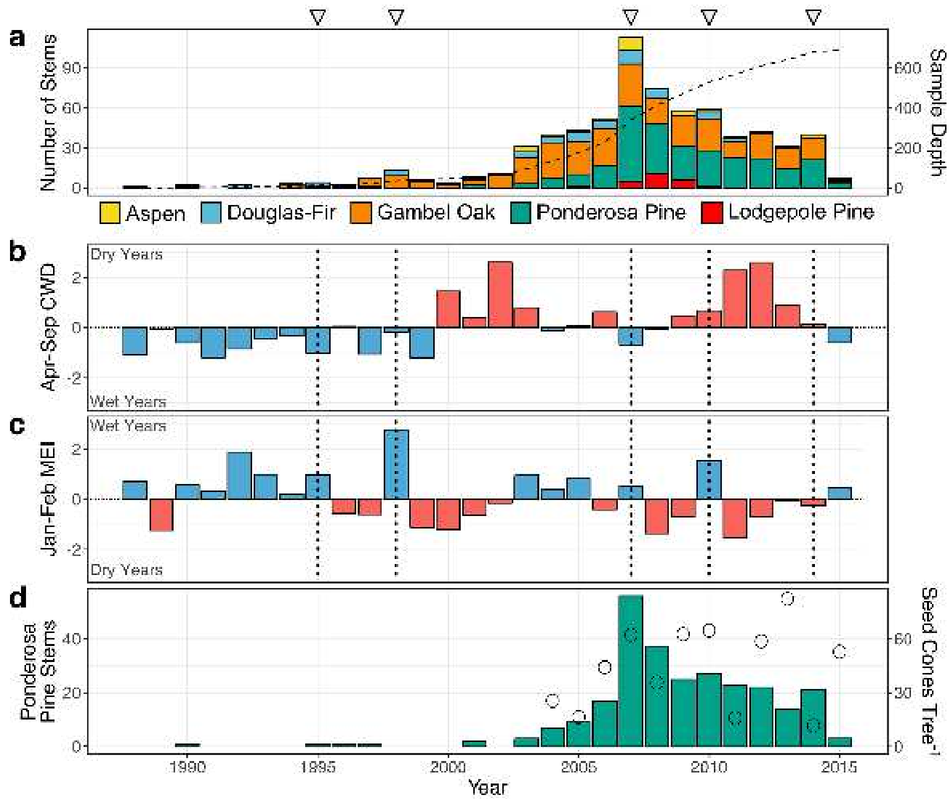

eap_2001_f4.tif

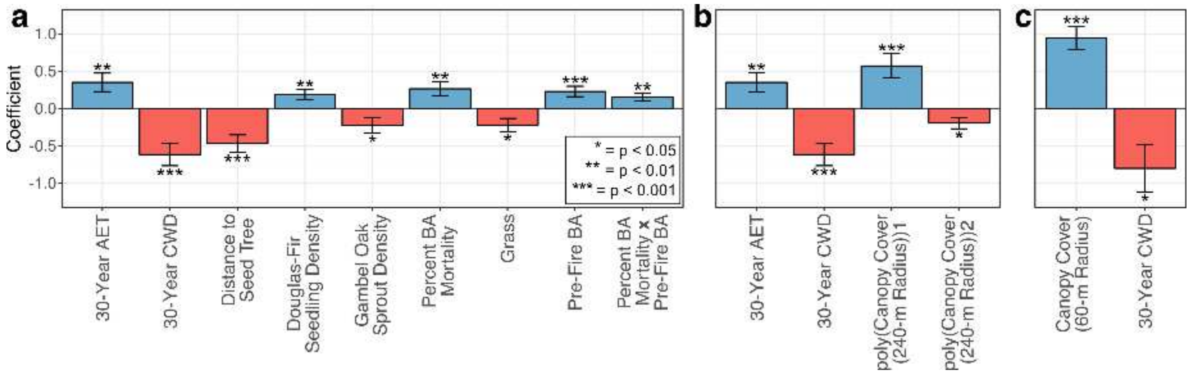

eap_2001_f5.tif

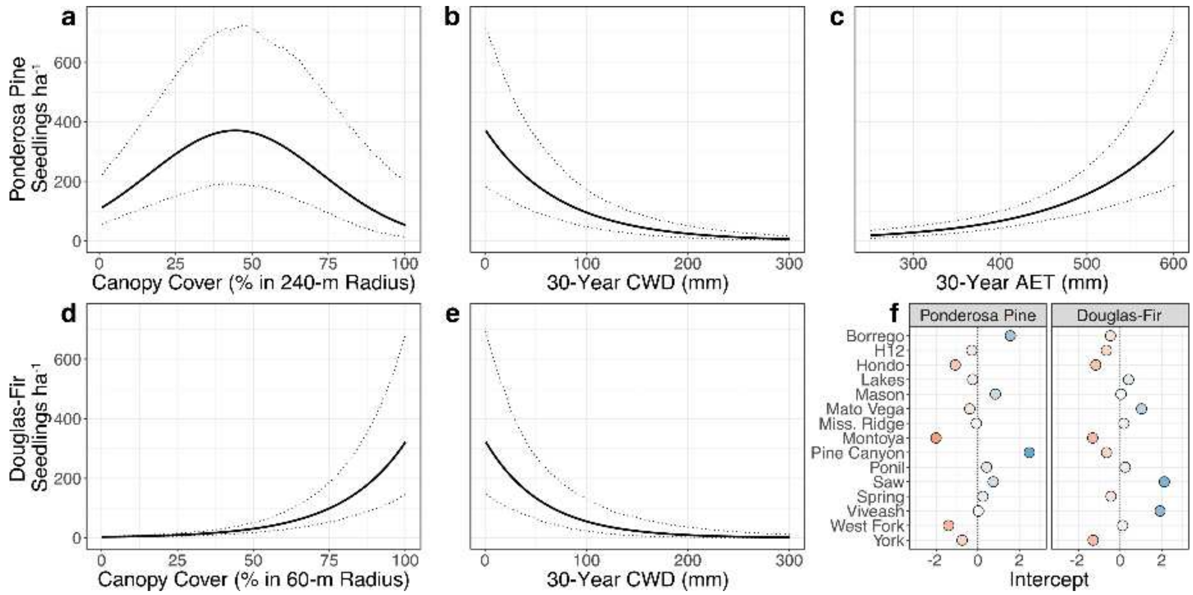

eap_2001_f6.tif

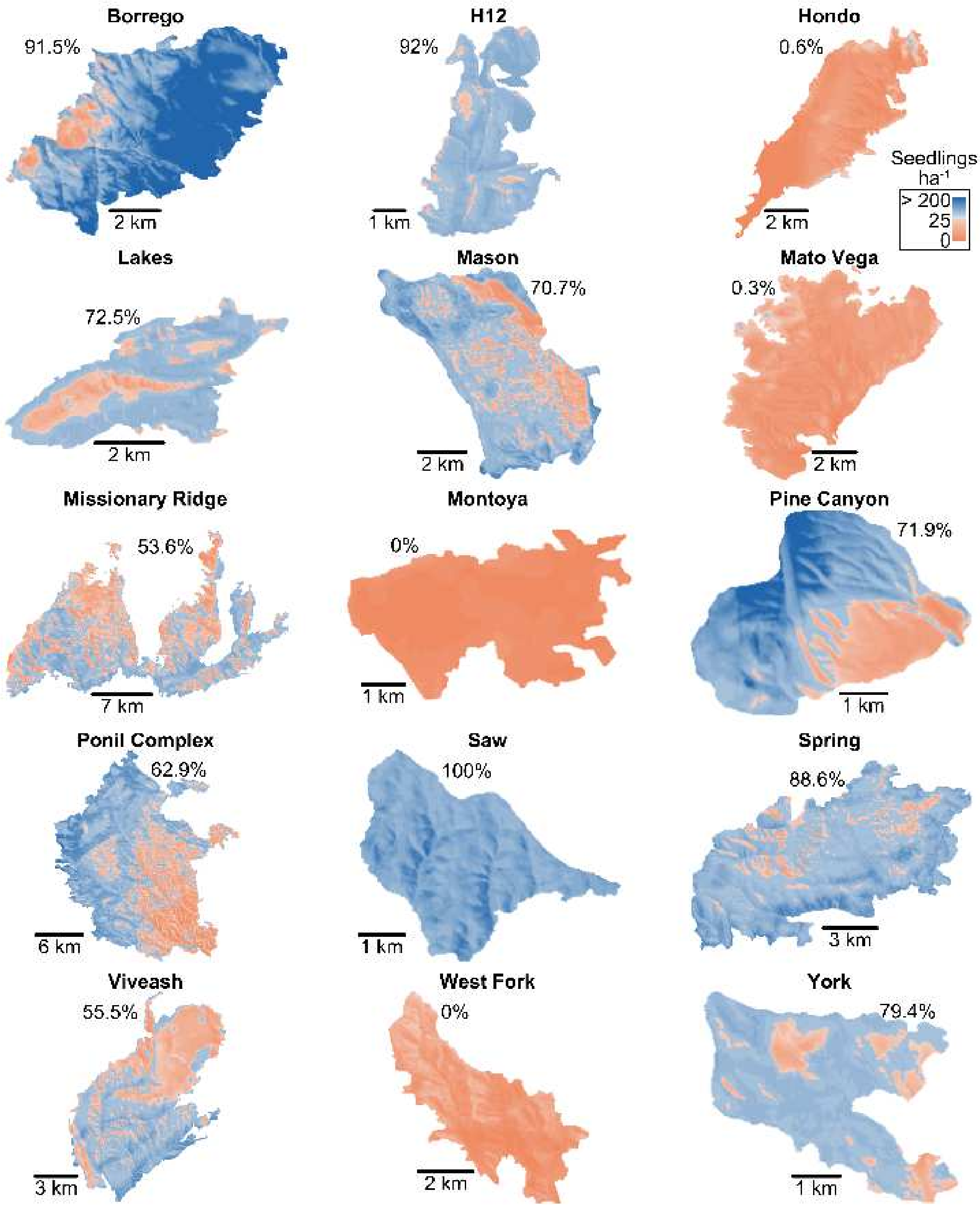

eap_2001_f7.tiff

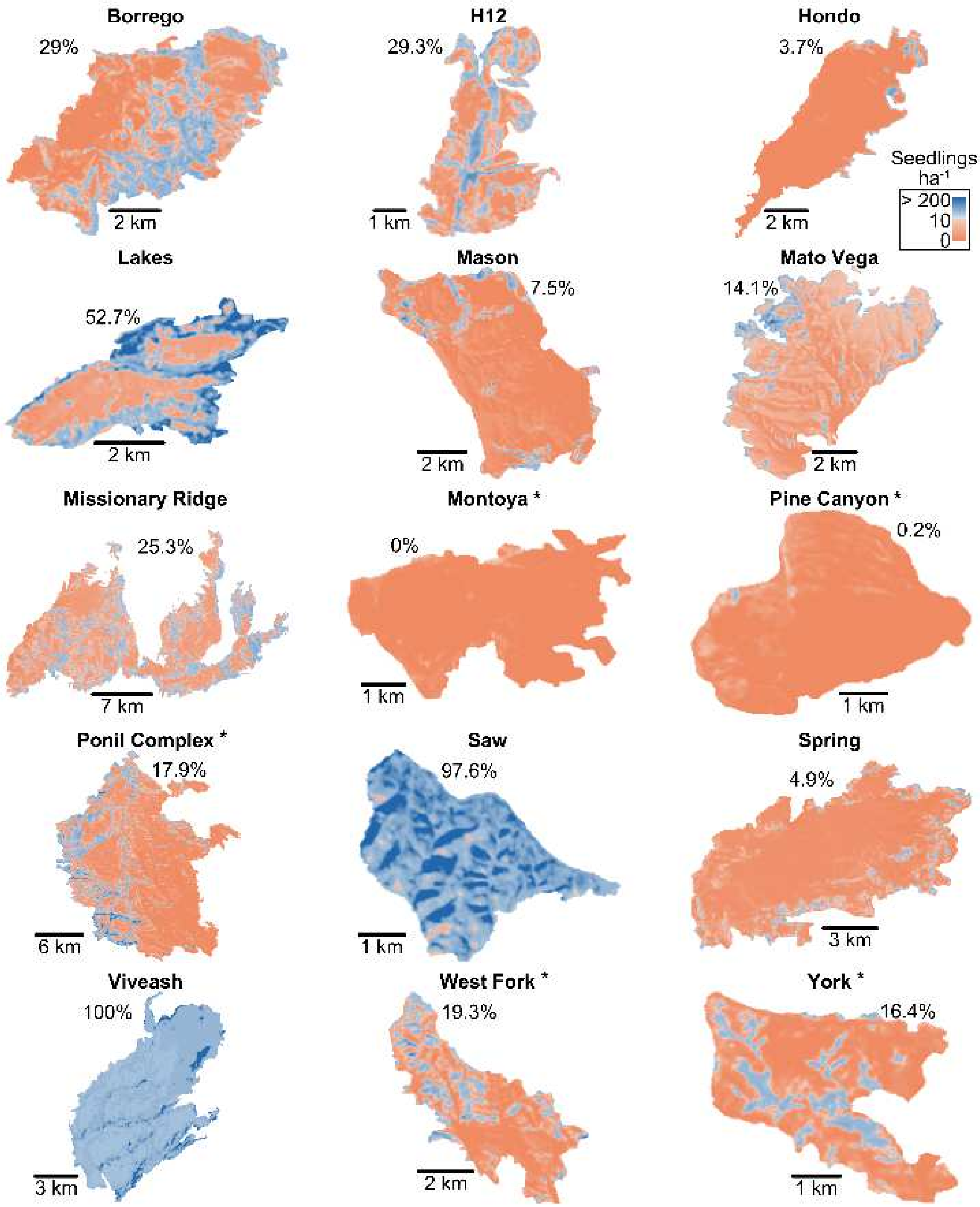

eap_2001_f8.tiff